Applied Biochemistry and Biotechnology (2019) 189:424–436
https://doi.org/10.1007/s12010-019-03022-0

Structural Modifications and Solution Behavior of Hyaluronic Acid Degraded with High pH and Temperature

Bruna Alice Gomes de Melo[1] · Maria Helena Andrade Santana[1]

Received: 13 February 2019 / Accepted: 22 April 2019 /
Published online: 2 May 2019

Abstract
Hyaluronic acid (HA) is a macromolecule with valuable benefits over its range of molar masses (MM). Degradation studies are relevant to maintain the same purity level in biomedical studies when using HA of different MM. We degraded HA via high pH and temperature and evaluated its MM, solution behavior, and structure over time. After 24 h, low MM HA was predominant, and the MM decreased from 753 to 36.2 kDa. Dynamic light scattering (DLS) showed a decrease in the number of HA populations, and the solution tended to be less polydispersed. The zeta potential varied from − 10 to − 30 mV, close to the stable range. FTIR showed that the primary structure of HA was affected after only 48 h of reaction. These results are relevant for the production of low MM HA to be used or mixed with high MM HA, generating structured biomaterials for biomedical applications.

Keywords Hyaluronic acid · Depolymerization · Low molar mass · Alkaline hydrolysis · Thermal degradation

Introduction

Hyaluronic acid (HA) is a glycosaminoglycan (GAG) that exists in a wide range of molar masses (MM) from < 10 to > 1000 kDa. It is a natural polysaccharide with repeated disaccharides containing one D-glucuronic acid and one n-acetyl-D-glucosamine, linked by β(1–3′) and β(1′-4) binding. In nature, HA exists in mammalian skin, eye vitreous humor, and the synovial fluid surrounding joints, promoting elasticity and lubrication [1]. This property is due to the high MM (> 1000 kDa) of this HA [2], which gives it high viscoelasticity.

In vivo, low MM HA (< 100 kDa) is a product of polysaccharide degradation, mediated by the endoglycosidase hyaluronidase enzyme [3]. The result of this degradation, as observed by

✉ Maria Helena Andrade Santana
mariahelena.santana@gmail.com

[1] Department of Engineering of Materials and Bioprocesses, School of Chemical Engineering, University of Campinas, P.O. Box 6066, Campinas, SP 13083-852, Brazil

West et al. [4], is a series of mechanisms that lead to angiogenic activities. This evidence has raised many questions about the importance of low MM HA and oligo-HA in the healing process, increasing the number of works concerning the potential applications and use of LMM HA [5]. However, this number is still not as expressive as that of studies involving high MM HA.

The stimulation of endothelial cell proliferation and migration [6], the expression of inflammatory cytokines [7], and the production of different types of collagen [8] give low MM HA the ability to stimulate wound healing and tissue repair [9–11]. Besides, it assumes a chondroprotective role by forming a layer around chondrocytes, preventing them from interacting with free radicals and metalloproteinases degradation [12]. Their smaller molecules penetrate cartilage cavities that high MM HA is unable to, preserving chondrocyte integrity [13]. Therefore, the use of mixed HA could be advantageous, as observed by Petrella et al. [14], in which patients treated with a combination of high and low MM HA showed improvements in osteoarthritis treatment.

Currently, commercial HA is available in different MM, with their production deriving from different sources such as microorganism fermentation and animal extraction. However, to obtain HA with a wide range of MM maintaining the same purity level, studies involving HA cleavage are becoming important.

The polysaccharide can be cleaved by different mechanisms using biological, chemical, and physical agents [15]. Biologically, HA is degraded by hyaluronidase enzymes, as mentioned above, and it provides fragments and products that occur physiologically [16]. The options for chemical and physical degradation are numerous and are the most used methods in the literature. HA can be cleaved hydrolytically, as shown by Tokita and Okamoto [17] in pioneering work that elucidated the mechanisms for the acidic and alkaline hydrolysis of HA. Since then, other works have studied the effects of pH on HA degradation and rheological properties [18–20]. HA can be degraded through exposition to reactive oxygen species, which are also responsible for its physiological depolymerization and occur from various pathways and sources, including exposition to ultraviolet (UV) light irradiation [21]. In addition to these methods, high-temperature treatments [22, 23], ultrasonication [24, 25], ozone [26], electron beam [27], gamma ray, and microwave irradiation [28] also decreased HA MM. Simulescu et al. [29] reported that HA degraded only after being stored at room temperature for 2 months and they observed that the lower the initial MM, the greater the degradation.

Concerning the quantification of HA MM, a conventional method is measuring the intrinsic viscosity ([η]) [30, 31], which assumed that HA has a coil configuration according to the Mark–Houwink–Kuhn–Sakurada equation. Currently, size exclusion chromatography, in tandem with multi-angle laser light scattering (SEC-MALLS), has been the most commonly used method to determine HA MM and its polymolecularity or polydispersity [32].

In this work, we aimed to produce low MM HA from the larger polysaccharide in order to obtain HA of different MM useful for biomedical studies and HA formulations. In addition to the controlled degradation, the control of purity degree in high and low MM is crucial for the mentioned applications. Here, we combined high temperature and high pH to cleave HA, two known methods for controlled degradation. As previously reported, at 60 °C, the chain's scission can be assured, but only even higher temperatures provide faster degradation [23]. Similarly, HA degradation under the alkaline condition is significant only at extreme pH (13) and long times, as verified by Maleki et al. [19]. Therefore, we intended to combine both

methods, high temperature (60 °C) and pH (12), to study HA degradation kinetics, aiming to optimize the time of low MM HA production. As mentioned above, Tokita and Okamoto [17] first described the mechanisms for hydrolytic cleavage of HA at 40 and 60 °C, showing that the rate of degradation increased at the higher temperature.

The originality of this study consists in investigating the degradation of HA with high pH and temperature from the decrease in its MM with time and of its colloidal behavior during the degradation process. Thus, we intended to present to the readers an in-depth view of the phenomena that occur in the system during degradation. For this, we used size exclusion chromatography (SEC) to obtain the MM distribution, and dynamic light scattering (DLS) techniques to evaluate the hydrodynamic diameter distribution, polydispersity index (PdI) and zeta potential of the entangled HA coils. Fourier transformed infrared (FTIR) spectroscopy was used to analyze the structure of the degraded HA over time.

Materials and Methods

Materials

HA (MM > 100 kDa) was purchased from Spec-Chem Ind. (Nanjing, China). All other reagents were purchased from Merck unless otherwise specified. Ultrapure water was used throughout all the experimental studies.

Determination of HA Purity Relative to the Protein Concentration

The purity of HA was calculated relative to the concentration of protein, as we previously reported [33]. HA concentration was determined by the cetyltrimethylammonium bromide turbidimetric method (CTAB), as described by Chen and Wang [34]. For protein quantification, the bicinchoninic acid (BCA) protein assay kit was used, based on the method proposed by Smith et al. [35]. Experiments were performed at 25 °C. The percentage of purity was calculated according to Eq. 1. The experiment was performed in triplicate.

$$\text{Purity}\ (\%) = \frac{C_{\text{HA}}}{(C_{\text{HA}} + C_{\text{P}})}.100 \tag{1}$$

where C_{HA} and C_{P} are the concentrations of the HA and soluble proteins, respectively.

HA Cleavage by Alkaline Hydrolysis and Temperature

To evaluate the effects of alkaline pH on HA cleavage, HA was dissolved in a pH 12 potassium chloride/sodium hydroxide buffer to obtain a 2 mg/mL solution. The buffer was prepared by mixing the appropriated portions of 0.2 mol/L KCl and 0.2 mol/L NaOH. The solution was placed in mechanical agitation (500 rpm) in a water bath at 60 °C, and aliquots were collected at different times: 0 (immediately after preparation) (HA-0), 1 h (HA-1), 5 h (HA-5), 8 h (HA-8), 24 h (HA-24), 48 h (HA-48), and 72 h (HA-72). HA prepared in phosphate-buffered saline (PBS), pH 7.4 was used as a control (HAc). Similar ionic strength was assured in all HA solutions.

Determination of HA MM

MM of the HAc and the degraded HA was determined by SEC in a Shimadzu chromatography system (Shimadzu Corporation, Kyoto, Japan), using a Polysep-GFC-P column guard (35 × 7.8 mm) (Phenomenex, Torrance, CA, USA) connected to a Polysep-GFC-P6000 gel filtration column (300 × 7.8 mm) (Phenomenex, Torrance, CA, USA). HA detection was performed by a Shimadzu RID-6A refractive index detector (Shimadzu Corporation, Kyoto, Japan). Samples were injected (20 μL) using 0.1 mol/L $NaNO_3$ as the mobile phase at a flow rate of 1 mL/min at 25 °C. Dextran (American Polymer Standards Corporation, Mentor, USA) was used as an indirect standard to estimate HA MM, as previously reported [36–38]. The experiment was performed in triplicate. The retention time of protein was previously determined by injecting soy protein in the equipment in order to exclude its interference in the chromatogram [33].

Viscosity Measurements

The viscosities of the control and degraded samples were measured at 25 °C using an A&D Vibro Viscometer SV-10 (A&D Company, Tokyo, Japan), by detecting the electric driving current of the solutions at a constant frequency of 30 Hz and amplitude < 1 mm.

Hydrodynamic Diameter, Polydispersity, and Zeta Potential Measurements

The DLS technique was used to measure the hydrodynamic diameter, PdI, and zeta potential of the HAc and the degraded HA, in an Autosizer 4700, Zetasizer Nano (Malvern Instruments, Malvern, UK) at 25 °C.The equipment measured each sample ten times.

FTIR Analysis

Samples were lyophilized in a lyophilizer L-101 (Liotop, São Carlos, Brazil) for 3 days. FTIR analyses of the solid HA were performed in a Thermo Scientific Nicolet 6700 spectrophotometer (Thermo Fisher Scientific, Madison, USA), using the single-reflection germanium attenuated total reflection (ATR) technique, in a Smart OMNI-Sampler (Thermo Fisher Scientific, Madison, USA). The wavelength range of the performance was 4000–750 cm^{-1} with a resolution of 4 cm^{-1}.

Statistical Analysis

Data were expressed as the mean ± SD obtained from three independent experiments. When relevant, one-way analysis of variance (ANOVA) with Tukey's test was used for statistical analysis. A 95% confidence level was considered significant ($p \leq 0.05$).

Results and Discussion

Distribution of HA MM with Time Reaction

The purity of HA was calculated relative to the concentration of protein (0.154 ± 0.03 mg/mL), is 92.5 ± 1.2%. The chromatograms of the control and aliquots from different reaction times

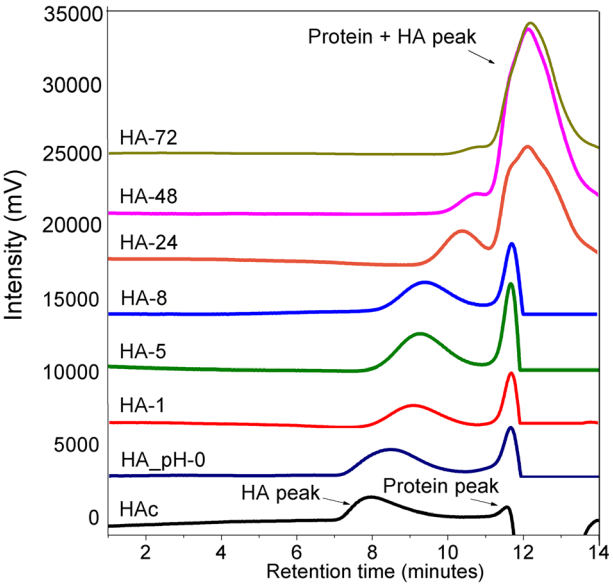

Fig. 1 Chromatograms of the HAc (pH 7.4, 25 °C), HA degraded at pH 12 and 25 °C (HA-0), and HA degraded at pH 12 and 60 °C under mechanical agitation for 1 (HA-1), 5 (HA-5), 8 (HA-8), 24 (HA-24), 48 (HA-48), and 72 h (HA-72) were obtained from the SEC analysis, showing the displacement of HA peaks with reaction time, which indicates the decrease of its MM

are presented in Fig. 1 and exhibit an elongated HA peak, between 7 and 10 min for HAc. This peak comprises the presence of three ranges of MM, as determined using dextran standards [39] corresponding to 34.8 ± 1.4% of HA 1000 kDa, 61.2 ± 1.5% of HA 100 kDa and 4.0 ± 0.1% of HA 10 kDa. After approximately 11 min, we observed a weak peak related to the presence of small amounts of protein.

By dissolving HA in the pH 12 buffer, we observed a progressive degradation over time. For sample HA-0, there was a slight displacement of the HA peak to the right, indicating a

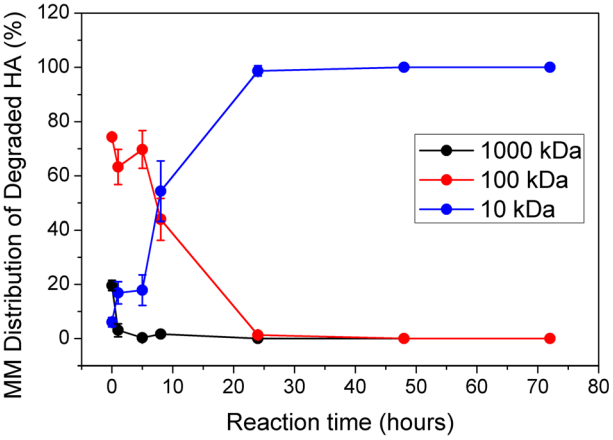

Fig. 2 Degradation kinetics of HA and its MM distribution, calculated from the SEC analysis. High and intermediate MM HA percentage decreased with time, whereas low MM HA increased, reaching the equilibrium in 24 h of reaction

Table 1 Average MM of HAc (pH 7.4, 25 °C), HA degraded at pH 12 and 25 °C (HA-0), and HA degraded at pH 12 and 60 °C under mechanical agitation for 1 (HA-1), 5 (HA-5), 8 (HA-8), 24 (HA-24), 48 (HA-48) and 72 h (HA-72). Values were calculated from the SEC analysis

Condition	MM (kDa)
HAc	753.2 ± 132.3
HA-0	597.7 ± 60.0
HA-1	43.1 ± 1.1
HA-5	41.5 ± 18.4
HA-8	36.2 ± 5.6
HA-24	36.2 ± 2.7
HA-48	36.3 ± 14.6
HA-72	25.4 ± 2.6

decrease in the HA with a higher MM. Under high temperature and after 1 h of reaction (HA-1), the displacement of the HA peak became more pronounced, whereas the protein peak increased in intensity. This effect is due to the formation of low MM HA and other fragments whose retention time is located in the same region as the proteins, causing overlapping of the peaks. The overlapping became more intense after 24 h of reaction (HA-24 to HA-72), indicating predominantly low MM HA.

The quantitative data of the HA MM distribution is shown in Fig. 2. Significant changes occur in the first hour of reaction, with high MM HA showing a fast degradation, and decreasing its content from 19.6 ± 1.9% to 3.1 ± 2.3%, while intermediate MM HA decreased from 74.3 ± 0.1% to 63.3 ± 6.5%, and low MM HA increased from 6.1 ± 1.8 to 16.9 ± 4.1%. After 8 h, the amount of 100 kDa HA decreased to 43.9 ± 7.7% at the same time that the low MM HA percentage increased to 54.4 ± 11.2%. Therefore, 8 h was the reaction time where we obtained a sample with almost equal portions of HA with the two different MM types. After 24 h, there was no significant changes in the high, intermediate, and high MM HA.

MM decreased when HA was in alkaline pH, from 753.2 ± 132.3 kDa (HAc) to 597.7 ± 60.0 (HA-0); however, a more significant change was obtained after 1 h of reaction at 60 °C,

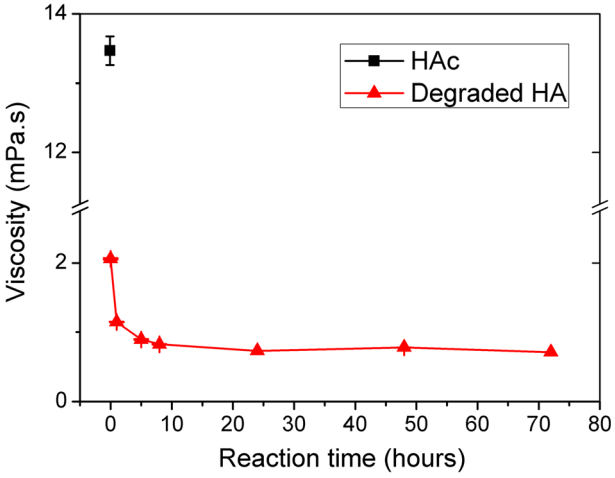

Fig. 3 Viscosity of HAc (pH 7.4, 25 °C), HA degraded at pH 12 and 25 °C (HA-0), and HA degraded at pH 12 and 60 °C under mechanical agitation for 1 (HA-1), 5 (HA-5), 8 (HA-8), 24 (HA-24), 48 (HA-48), and 72 h (HA-72), measured at 25 °C

with MM decreasing to 43.1 ± 1.1 kDa (HA-1) and reaching 25.4 ± 2.6 kDa after 72 h (HA-72), as shown in Table 1. These results evidenced the positive effect of high temperature on a faster alkaline degradation of HA molecules. Therefore, the combination of pH 12 and 60 °C provided a synergistic effect of hydrolytic and thermal degradation, resulting in an irreversible change in the HA MM fractions, which was more expressive than the isolated effects of pH or temperature as usually reported in the literature [40].

According to Morris et al. [41], an alkaline condition results in a reversible decrease in viscosity, suggesting a non-covalent breakage of chains due to the reduction of intramolecular H bonds. This was observed by Maleki et al. [19], which studied the effects of a wide range of pH values on HA structure, varying from 1 to 13, and observed that after 24 h of reaction, only at the extreme pH values (1 and 13) an irreversible degradation occurred, especially at pH 13. Here, results strongly suggest the irreversible cleavage of HA chains, due to the synergistic effect of pH 12 and 60 °C, once both viscosity and MM significantly decreased after 1 h of reaction.

Effects of Time Reaction on HA Viscosity

Viscosity is proportional to the polymer's MM due to the physical cross-linking from the entanglement of their chains [25]. However, degradation is a kinetic process with initial and intermediate steps that do not affect MM immediately. As observed by Gatej et al. [18], even for a substantial decrease in the viscosity of the HA solution at pH to 12.6, the MM was only slightly changed. From these results, the authors concluded that a reversible decrease in HA stiffness occurred, due to intra- and intermolecular cleavage of the hydrogen bonds [41, 42]. Here, results showed the reversible behavior of HA-0, followed by an irreversible chains cleavage from 1 h of reaction at pH 12 and 60 °C, with viscosity dropping to 1.15 ± 0.01 mPa s, and stabilizing in 24 h around 1 mPa s (Fig. 3), presenting viscosity values similar to that of water [43].

Hydrodynamic Diameter Distribution, Polydispersity, and Zeta Potential of the HA

In solutions with a concentration above 1 mg/mL, HA randomly entangles forming elongated coil structures [44]. By the DLS technique, we verified the hydrodynamic diameter of these entanglements using the intensity distribution (Fig. 4), which is proportional to the diameter to the sixth power (Iαd6).

Figure 4a (i) shows the diameter distribution of the control (HAc), where we observed a large variety of populations, from 1 to 5000 nm, which is likely due to the presence of HA with different MM, as shown in "Distribution of HA MM with Time Reaction," and added to the random aggregation of the coils. The PdI value corroborates this result, which is close to 1 (0.88 ± 0.04), indicating the sample was highly polydispersed (Fig. 4c).

Figure 4a (ii) and (iii) show HA in the alkaline medium. From time zero, we observed a restructuration of the coil entanglements, probably due to the effects of the hydrogen bond cleavage. According to Ghosh et al. [42], this cleavage leads to a contraction of the coils, which would result in a size decrease. Here, we observed that the 5000-nm population in HAc is not present, indicating that they may have contracted and formed smaller structures. At the same time, the 1- and 5-nm populations were also not observed, likely due to aggregation. Figure 4a (ii) shows a more

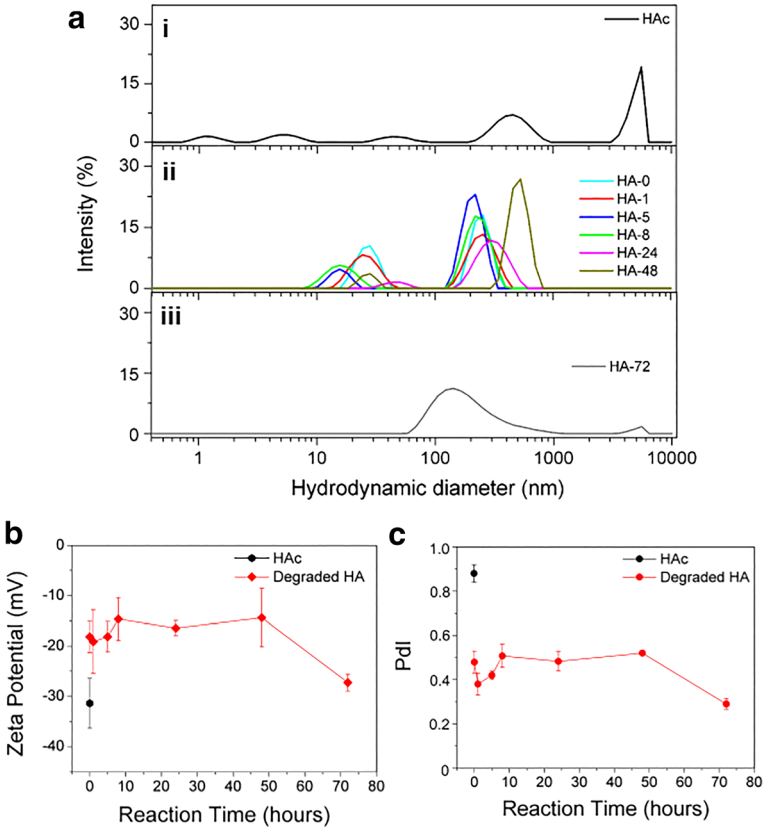

Fig. 4 **a** Intensity distribution of the hydrodynamic diameter of (i) HAc (pH 7.4, 25 °C); (ii) HA degraded at pH 12 and 25 °C (HA-0), and HA degraded at pH 12 and 60 °C for 1 (HA-1), 5 (HA-5), 8 (HA-8), 24 (HA-24), and 48 h (HA-48); and (iii) HA degraded at 72 h (HA-72). **b** zeta potential and **c** PdI of HAc and degraded HAs. Results were obtained from DLS analysis at 25 °C

organized environment, with the presence of only two populations of 10–50 nm and 100–400 nm, resulting in a decrease of PdI of almost twofold, corresponding to 0.48 ± 0.05 for HA-0, 0.38 ± 0.05 for HA-1, 0.42 ± 0.02 for HA-5, 0.51 ± 0.05 for HA-8, 0.48 ± 0.04 for HA-24, and 0.52 ± 0.01 for HA-48 (Fig. 4c).

The hydrodynamic diameter distribution of HA-72 (Fig. 4a (iii)), shows only one broad peak for the population with a 100-nm mean diameter, different from the lower reaction times. Similar to the sample HA-48, there was a complete degradation of the high and intermediate MM HA, forming HA of 10 kDa. However, after only 72 h, the coils seem to have self-organized into one entanglement, which decreased the PdI to 0.29 ± 0.02 (Fig. 4c).

When in a neutral solution, the carboxyl groups of the HA are deprotonated, which leads to electrostatic repulsion, favoring the formation of structures with coils that are distant from each other and have a high level of hydration [45, 46]. With the increase of pH, the net HA charge increases, which contributes to the destabilization of the hydrogen bond network and causes aggregation [18].

To evaluate variations in the HA net charge, we analyzed the zeta potential of the samples. Zeta potential is commonly used to assess ionic charge exposition and to estimate colloidal

stability by electrostatic repulsion, preventing aggregation. Therefore, the recommended levels of zeta potential for long-term stability are higher than 30 mV or lower than − 30 mV [47]. Zeta potential is a valuable parameter for understanding HA behavior in a solution and determining stability after degradation. However, few works in the literature describe results from this analysis. Mondek et al. [23] observed that after 12 h at 60 °C, the zeta potential of HA changed only slightly and remained below − 30 mV, which is stable and resistant to aggregation.

For our control, i.e., pH 7.4, the zeta potential was − 31.4 ± 5.0 mV, within the stable range, due to the polyanionic character of HA in neutral medium. The results for the diameter distribution exhibited an aggregation of entanglements in the alkaline medium, which was likely due to the structural changes during the degradation process. This result corroborates with our zeta potential values, which tended to increase from 0 (− 18.3 ± 3.1 mV) to 48 h (− 14.3 ± 5.8 mV) during the initial and intermediate steps of degradation, resulting in changes of conformation and less exposition of the COO– groups. After 48 h of reaction, intermediate structures were modified due to the complete chain scission and more exposition of COO– groups, resulting in a decrease in the zeta potential to −27.2 ± 1.7 mV for HA-72 (Fig. 4b) [23]. These structures were electrostatically stable coils of 100 to 1000 nm with low PDI (Fig. 4c).

FTIR Analysis

After investigating the effects of pH, temperature and reaction time on the MM distribution and HA entanglement behavior in solution, we performed an FTIR analysis to more accurately examine the changes in the HA structure. Figure 5 shows the spectra of HAc and the degraded samples. The transmission bands were interpreted according to Günzler and Gramlich [48].

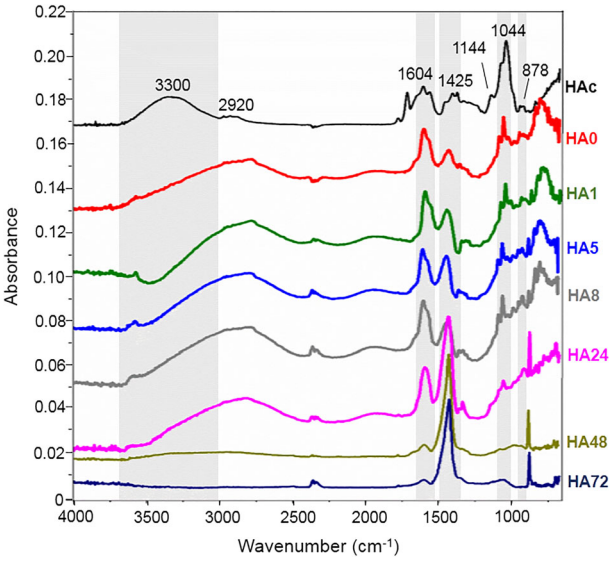

Fig. 5 FTIR spectra of the HAc (pH 7.4, 25 °C), HA degraded at pH 12 and 25 °C (HA-0) and HA degraded at pH 12 and 60 °C for 1 (HA-1), 5 (HA-5), 8 (HA-8), 24 (HA-24), 48 (HA-48), and 72 h (HA-72). The main peaks are highlighted to better visualize the displacements and intensity changes caused by degradation. Data were vertically shifted to avoid overlapping

For the control, specific bands of HA were observed [49], as also noted by Choi et al. [27], in which HA purity was around 95%, a similar level to that used in this work. Here, we observed a broad peak from 3600 to 3000 cm^{-1}, which is characteristic of the O–H stretching band of aqueous solutions, and C–O and N–H HA stretching bands. A less intense peak was observed at 2904 cm^{-1}, corresponding to the C–H vibration. At a high pH for samples HA-0 to HA-24, there was a displacement of the hydroxyl peak to a lower wavenumber, overlapping the alkane band. This displacement suggests the formation of strong O–H bonds between the water molecules and Na^+ cations [50]. For sample HA-48, the intensity of this broad peak significantly decreased, and for HA-72, it was nonexistent, showing that long periods in high pH conditions may have caused modifications to the primary structure of the HA molecules.

At 1604 cm^{-1}, we observed the peak corresponding to the C=O stretching band of the amide, which decreased in intensity after 48 h of reaction. At 1425 cm^{-1}, the peak of the carboxyl C–O stretching band increased with time, indicating the formation of carboxylic acid groups during degradation. The shoulder at 1144 cm^{-1} in the control suggests the C–O–C stretching band, and the peak at 1042.49 cm^{-1} to C–C–O stretching, which significantly decreased in the HA at an alkaline pH. Finally, at 878 cm^{-1}, we observed a peak in the degraded samples that became more intense after 24 h, corresponding to out-of-ring deformations (C–O–H, C–C–H, and O–C–H). The results obtained from the FTIR analysis showed that time strongly affected the HA primary structure, indicating that under the conditions used in this work, the reaction time should be no longer than 24 h to achieve low MM HA without compromising the molecule.

Conclusions

HA progressively degraded with time when dissolved in an alkaline buffer at high temperature. The results showed that after 8 h of reaction, low MM HA predominated, being the only HA present in the solution after 2 days. We observed that the viscosity sharply decreased initially. From the MM distribution, we concluded that this rheological parameter did not vary only with the decrease of MM but also due to the intra- and intermolecular cleavage of the hydrogen bonds. This cleavage resulted in structural changes and a reorganization of coil entanglements, as observed in the hydrodynamic diameter distribution, which contributed to a less polydispersed solution. The zeta potential indicated that the lower the polydispersity, the more stable the HA entanglements tended to be. Finally, from the FTIR analysis, we verified that the degradation processes compromised the primary structures of the HA after only 48 h. In this work, we showed the synergistic effect of high temperature and pH on a fast degradation of HA, producing low MM HA with low polydispersity that was stable concerning aggregation. This method can allow fabrication of HA of different MM that maintains the same level of purity for medical, pharmaceutical, and cosmetic studies. Further studies should focus on the degradation kinetics of HA using different pH and temperatures.

Funding information This study was financially supported by Fapesp (São Paulo Research Foundation), grant numbers 2015/23134-8 and 2016/10132-0.

Compliance with Ethical Standards

Conflict of Interest The authors declare that they have no conflicts of interest.

References

1. Garg, H. G., & Hales, C. A. (2004). *Chemistry and biology of hyaluronan*. Elsevier.
2. Lee, H. G., & Cowman, M. K. (1994). An agarose gel electrophoretic method for analysis of hyaluronan molecular weight distribution. *Anal.Biochem., 219*(2), 278–287.
3. Slevin, M., Kumar, S., & Gaffney, J. (2002). Angiogenic oligosaccharides of hyaluronan induce multiple signaling pathways affecting vascular endothelial cell mitogenic and wound healing responses. *The Journal of Biological Chemistry, 277*(43), 41046–41059. https://doi.org/10.1074/jbc.M109443200.
4. West, D. C., Hampson, I. N., Arnold, F., & Kumar, S. (1985). Angiogenesis induced by degradation products of hyaluronic acid. *Science., 228*(4705), 1324–1326.
5. R. Stern, A. a. Asari, K.N. Sugahara, Hyaluronan fragments: an information-rich system, European Journal of Cell Biology 85 (2006) 699–715. https://doi.org/10.1016/j.ejcb.2006.05.009., 8
6. Sattar, A., Kumar, S., & West, D. C. (1992). Does hyaluronan have a role in endothelial cell proliferation of the synovium? *Seminars in Arthritis and Rheumatism, 22*(1), 37–43. https://doi.org/10.1016/0049-0172(92)90047-H.
7. P.W. Noble, Hyaluronan and its catabolic products in tissue injury and repair, Matrix Biol. 21 (2002) 25–29. https://doi.org/10.1146/annurev.cellbio.23.090506.123337.
8. Rooney, P., Wang, M., Kumar, P., & Kumar, S. (1993). Angiogenic oligosaccharides of hyaluronan enhance the production of collagens by endothelial cells. *Journal of Cell Science, 105*(Pt 1), 213–218 http://www.ncbi.nlm.nih.gov/pubmed/7689574.
9. Gao, F., Liu, Y., He, Y., Yang, C., Wang, Y., Shi, X., & Wei, G. (2010). Hyaluronan oligosaccharides promote excisional wound healing through enhanced angiogenesis. *Matrix Biology, 29*(2), 107–116. https://doi.org/10.1016/j.matbio.2009.11.002.
10. Schlesinger, T., & Powell, C. R. (2012). Efficacy and safety of a low-molecular weight hyaluronic acid topical gel in the treatment of facial seborrheic dermatitis final report. *J. Clin. Aesthetic Dermatology., 7*, 15–18.
11. Shewale, A. R., Barnes, C. L., Fischbach, L. A., Ounpraseuth, S., Painter, J. T., & Martin, B. C. (2017). Comparative effectiveness of low, moderate and high molecular weight hyaluronic acid injections in delaying time to knee surgery. *The Journal of Arthroplasty, 32*(17), 2952–2957. https://doi.org/10.1016/j.apsusc.2009.03.091.
12. Ghosh, P., & Guidolin, D. (2002). Potential mechanism of action of intra-articular hyaluronan therapy in osteoarthritis: are the effects molecular weight dependent? *Seminars in Arthritis and Rheumatism, 32*(6), 10–37. https://doi.org/10.1053/sarh.2002.32549.
13. Euppayo, T., Siengdee, P., Buddhachat, K., Pradit, W., Viriyakhasem, N., Chomdej, S., Ongchai, S., Harada, Y., & Nganvogpanit, K. (2015). Effects of low molecular weight hyaluronan combined with carprofen on canine osteoarthritis articular chondrocytes and cartilage explants in vitro. *In Vitro Cellular & Developmental Biology. Animal, 51*(8), 857–865. https://doi.org/10.1007/s11626-015-9908-9.
14. Petrella, R. J., Decaria, J., & Petrella, M. J. (2011). Long term efficacy and safety of a combined low and high of osteoarthritis of the knee. *Rheumatol. Reports., 3*(1), 4. https://doi.org/10.4081/rr.2011.e4.
15. Stern, R., Kogan, G., Jedrzejas, M. J., & Šoltés, L. (2007). The many ways to cleave hyaluronan. *Biotechnology Advances, 25*(6), 537–557. https://doi.org/10.1016/j.biotechadv.2007.07.001.
16. Cardoso, M. J., Caridade, S. G., Costa, R. R., & Mano, J. F. (2016). Enzymatic degradation of polysaccharide-based layer-by-layer structures. *Biomacromolecules., 17*(4), 1347–1357. https://doi.org/10.1021/acs.biomac.5b01742.
17. Tokita, Y., & Okamoto, A. (1995). Hydrolytic degradation of hyaluronic. *Polymer Degradation and Stability, 48*(2), 269–273.
18. Gatej, I., Popa, M., & Rinaudo, M. (2004). Role of the pH on hyaluronan behavior in aqueous solution. *Biomacromolecules., 6*(1), 61–67. https://doi.org/10.1021/bm040050m.
19. Maleki, A., Kjøniksen, A. L., & Nyström, B. (2008). Effect of pH on the behavior of hyaluronic acid in dilute and semidilute aqueous solutions. *Macromolecular Symposia, 274*(1), 131–140. https://doi.org/10.1002/masy.200851418.
20. Tømmeraas, K., & Melander, C. (2008). Kinetics of hyaluronan hydrolysis in acidic solution at various pH values. *Biomacromolecules., 9*(6), 1535–1540. https://doi.org/10.1021/bm701341y.

21. Šoltés, L., Mendichi, R., Kogan, G., Schiller, J., Stankovská, M., & Arnhold, J. (2006). Degradative action of reactive oxygen species on hyaluronan. *Biomacromolecules., 7*(3), 659–668. https://doi.org/10.1021/bm050867v.
22. Caspersen, M. B., Roubroeks, J. P., Liu, Q., Huang, S., Fogh, J., Zhao, R., & Tømmeraas, K. (2014). Thermal degradation and stability of sodium hyaluronate in solid state. *Carbohydrate Polymers, 107*, 25–30. https://doi.org/10.1016/j.carbpol.2014.02.005.
23. Mondek, J., Kalina, M., Simulescu, V., & Pekař, M. (2015). Thermal degradation of high molar mass hyaluronan in solution and in powder; comparison with BSA. *Polymer Degradation and Stability, 120*, 107–113. https://doi.org/10.1016/j.polymdegradstab.2015.06.012.
24. Dřímalová, E., Velebný, V., Sasinková, V., Hromádková, Z., & Ebringerová, A. (2005). Degradation of hyaluronan by ultrasonication in comparison to microwave and conventional heating. *Carbohydrate Polymers, 61*(4), 420–426. https://doi.org/10.1016/j.carbpol.2005.05.035.
25. Gura, E., Hückel, M., & Müller, P.-J. (1998). Specific degradation of hyaluronic acid and its rheological properties. *Polymer Degradation and Stability, 59*(1-3), 297–302. https://doi.org/10.1016/S0141-3910(97)00194-8.
26. Wu, Y. (2012). Preparation of low-molecular-weight hyaluronic acid by ozone treatment. *Carbohydrate Polymers, 89*(2), 709–712. https://doi.org/10.1016/j.carbpol.2012.03.081.
27. il Choi, J., Kim, J. K., Kim, J. H., Kweon, D. K., & Lee, J. W. (2010). Degradation of hyaluronic acid powder by electron beam irradiation, gamma ray irradiation, microwave irradiation and thermal treatment: a comparative study. *Carbohydrate Polymers, 79*(4), 1080–1085. https://doi.org/10.1016/j.carbpol.2009.10.041.
28. Chen, S., Chen, H., Gao, R., Li, L., Yang, X., Wu, Y., & Hu, X. (2015). Degradation of hyaluronic acid derived from tilapia eyeballs by a combinatorial method of microwave, hydrogen peroxide, and ascorbic acid. *Polymer Degradation and Stability, 112*, 117–121. https://doi.org/10.1016/j.polymdegradstab.2014.12.026.
29. Simulescu, V., Kalina, M., Mondek, J., & Pekař, M. (2016). Long-term degradation study of hyaluronic acid in aqueous solutions without protection against microorganisms. *Carbohydrate Polymers, 137*, 664–668. https://doi.org/10.1016/j.carbpol.2015.10.101.
30. Laurent, T. C., Ryan, M., & Pietruszkiewicz, A. (1960). Fractionation of hyaluronic acid. The polydispersity of hyaluronic acid from the bovine vitreous body. *Biochim. Biophys. Acta - Mol. Cell Res., 42*, 476–485.
31. Sun, J., Wang, M., Chen, Y., Shang, F., Ye, H., & Tan, T. (2012). Understanding the influence of phosphatidylcholine on the molecular weight of hyaluronic acid synthesized by Streptococcus zooepidemicus. *Applied Biochemistry and Biotechnology, 168*(1), 47–57. https://doi.org/10.1007/s12010-011-9320-1.
32. Schiraldi, C., Andreozzi, L., Marzaioli, I., Vinciguerra, S., D'Avino, A., Volpe, F., Panariello, A., & De Rosa, M. (2010). Hyaluronic acid degradation during initial steps of downstream processing. *Biocatalysis and Biotransformation, 28*(1), 83–89. https://doi.org/10.3109/10242420903408344.
33. Cavalcanti, A. D. D., Melo, B. A. G., & Oliveira, R. C. (2018). Recovery and purity of high molar mass bio-hyaluronic acid via precipitation strategies modulated by pH and sodium chloride. *Applied Biochemistry and Biotechnology*.
34. Chen, Y. H., & Wang, Q. (2009). Establishment of CTAB turbidimetric method to determine hyaluronic acid content in fermentation broth. *Carbohydrate Polymers, 78*(1), 178–181. https://doi.org/10.1016/j.carbpol.2009.04.037.
35. Smith, P. K., Krohn, R. I., Hermanson, G. T., Mallia, A. K., Gartner, F. H., Provenzano, M. D., Fujimoto, E. K., Goeke, N. M., Olson, B. J., & Klenk, D. (1985). Measurement of protein using bicinchoninic acid. *pdf, Anal. Chem., 150*, 76–85.
36. S.T. Balke, A.E. Hamielec, B.P. Leclair, S.L. Pearce, Gel permeation chromatography: calibration curve from polydisperse standards, I EC Prod. Res. Dev. 8 (1969) 54–57. https://doi.org/10.1021/i360029a008, 1.
37. Pires, A. M. B., & Eguchi, S. Y. (2010). The influence of mineral ions on the microbial production and molecular weight of hyaluronic acid. *Applied Biochemistry and Biotechnology, 162*(8), 2125–2135. https://doi.org/10.1007/s12010-010-8987-z.
38. Pan, N. C., Cristina, H., Pereira, B., De Lourdes, M., Flora, A., Vasconcelos, D., Antonia, M., & Colabone, P. (2017). Improvement production of hyaluronic acid by Streptococcus zooepidemicus in sugarcane molasses. *Applied Biochemistry and Biotechnology, 182*(1), 276–293. https://doi.org/10.1007/s12010-016-2326-y.
39. Pires, A. M. B., & Santana, M. H. A. (2011). Rheological aspects of microbial hyaluronic acid. *Journal of Applied Polymer Science, 122*(1), 126–133. https://doi.org/10.1002/app.33976.
40. Reháková, M., Bakoš, D., Soldán, M., & Vizárová, K. (1994). Depolymerization reactions of hyaluronic acid in solution. *International Journal of Biological Macromolecules, 16*(3), 121–124. https://doi.org/10.1016/0141-8130(94)90037-X.

41. Morris, E. R., Rees, D. A., & Welsh, E. J. (1980). Conformation and dynamic interactions in hyaluronate solutions. *Journal of Molecular Biology, 138*(2), 383–400.
42. Ghosh, S., Kobal, I., Zanette, D., & Reed, W. F. (1993). Conformational contraction and hydrolysis of hyaluronate in sodium hydroxide solutions. *Macromolecules., 26*(17), 4685–4693. https://doi.org/10.1021/ma00069a042.
43. Bothner, H., & Waaler, T. (1988). Limiting viscosity number and weight average molecular weight of hyaluronate samples produced by heat degradation. *International Journal of Biological Macromolecules, 10*(5), 287–291.
44. Laurent, T. C., Laurent, U. B., & Fraser, J. R. E. (1996). The structure and function of hyaluronan: an overview. *Immunology and Cell Biology, 74*(2), A1–A7. https://doi.org/10.1038/icb.1996.32.
45. Lapčík, L., Lapčík, L., De Smedt, S., Demeester, J., & Chabreček, P. (1998). Hyaluronan: preparation, structure, properties, and applications. *Chemical Reviews, 98*(8), 2663–2684. https://doi.org/10.1021/cr941199z.
46. Scott, J. E., & Heatley, F. (1999). Hyaluronan forms specific stable tertiary structures in aqueous solution: a 13 C NMR study. *Biochemistry., 96*(9), 4850–4855. https://doi.org/10.1073/pnas.96.9.4850.
47. Hunter, R. J., Ottewill, R. H., & Rowell, R. L. (1981). Preface. In *Zeta potential in colloid science* (3rd ed.). Academic Press. https://doi.org/10.1016/B978-0-12-361961-7.50004-3.
48. H. Günzler, H.-U. Gremlich, IR spectroscopy: an introduction, Wiley-VCH, 2002. ISBN: 978-3-527-28896-0.
49. Gilli, R., Kacuráková, M., Mathlouthi, M., Navarini, L., & Paoletti, S. (1994). FTIR studies of sodium hyaluronate and its oligomers in the amorphous solid phase and in aqueous solution. *Carbohydrate Research, 263*(2), 315–326. https://doi.org/10.1016/0008-6215(94)00147-2.
50. Madejová, J. (2003). FTIR technique in clay mineral studies. *Vibrational Spectroscopy, 31*(1), 1–10.